Vol. 22, No. 2, Summer, 2026, 33-46
DOI: 10.22055/ivj.2026.556170.2862
Journal Homepage: http://www.ivj.ir/

Original Article

Dimethyl itaconate attenuates ovarian histological changes and apoptosis, and improves sex hormone production in doxorubicin-treated 4T1 breast cancer mice

Azam Asad-Saftjani[1], Shima Hosseinifar[2*] and Mohammad Reza Tabandeh[3]

[1] PhD Student of Histology, Faculty of Veterinary Medicine, Shahid Chamran University of Ahvaz, Ahvaz, Iran
[2] Associate Professor, Department of Basic Sciences, Faculty of Veterinary Medicine, Shahid Chamran University of Ahvaz, Ahvaz, Iran
[3] Professor, Department of Basic Sciences, Faculty of Veterinary Medicine, Shahid Chamran University of Ahvaz, Ahvaz, Iran and Professor, Stem Cells and Transgenic Technology Research Center, Shahid Chamran University of Ahvaz, Ahvaz, Iran

Received: 29.10.2025 Accepted: 16.02.2026

Abstract

Ovarian toxicity induced by Doxorubicin (DOX) is a common side effect treatment in breast cancer, leading to apoptosis, impaired folliculogenesis and reduced ovarian steroid hormone levels. Dimethyl itaconate (DMI) is an immunometabolite with anti-inflammatory and antioxidant properties that could play a protective role, although data are limited. This study evaluated the potential protective effects of DMI on ovarian histology, apoptosis, and ovarian hormone production in a 4T1 breast cancer mouse model treated with DOX. In this study, 30 adult female BALB/c mice were randomly divided into five groups: healthy control, cancer control (cancer induction by injection of 4T1 cells), cancer - DMI (50 mg/kg; daily; IP, 28 days), cancer - DOX (5 mg/kg; once a week; IP, 4 weeks) and DMI + DOX cancer. Serum estrogen and progesterone levels, ovarian apoptotic gene expression (Bax and Bcl2), and histological changes were evaluated. Statistical analysis was performed by GraphPad Prism software (10) and data were presented as mean ± standard deviation. DOX significantly decreased estradiol (E2; 37.23 ± 4.43 pg/ml) and progesterone (P4; 3.4 ± 0.2 ng/ml) levels, reduced Bcl2 (0.31 ± 0.1) expression and increased Bax expression (4.04 ± 0.39) in ovarian tissue compared to cancer control group (54.10 ± 2.8 pg/ml, 5.1 ± 0.2 ng/ml; 0.72 ± 0.09; 1.81 ± 0.35, respectively). Co-treatment with DMI and DOX led to a significant decrease in Bax expression (2.59 ± 0.45) and a significant increase in Bcl-2 (0.61 ± 0.03) expression compared to the only DOX treated cancer group. DOX caused notable ovarian damage, including increased follicular atresia, reduced follicle size, and absence of corpus luteum. DMI treatment mitigated these effects by preserving ovarian architecture, thinning the surface epithelium, and normalizing hormone levels and expression of apoptosis-related genes. Co-administration of DMI and DOX was particularly effective in reducing DOX-induced histological damage. These findings suggest that DMI may serve as a potential protective compound for reducing DOX-induced ovarian toxicity during chemotherapy.

Key words: Dimethyl Itaconate, Doxorubicin, Ovarian histology, Apoptosis, Breast cancer

Introduction

Breast cancer is one of the most common malignancies among women, and with advancements in therapeutic strategies, patient survival rates have significantly improved. One major challenge in this context is the occurrence of premature ovarian failure (POF), resulting from chemotherapy-induced gonadotoxicity; a

[*] **Corresponding Author**: Shima Hosseinifar, Associate Professor, Department of Basic Sciences, Faculty of Veterinary Medicine, Shahid Chamran University of Ahvaz, Ahvaz, Iran
E-mail: sh.hosseinifar@suc.ac.ir

© 2020 by the authors. Licensee SCU, Ahvaz, Iran. This article is an open access article distributed under the terms and conditions of the Creative Commons Attribution-NonCommercial 4.0 International (CC BY-NC 4.0 license) (http://creativecommons.org/licenses/by-nc/4.0/).

process that impairs folliculogenesis and depletes the ovarian reserve (Yildiz et al, 2023). Among chemotherapeutic agents, doxorubicin (DOX) is widely used in the treatment of breast cancer. However, its high toxicity to healthy tissues, especially the ovaries, remains a significant concern (Bedoschi et al, 2016). DOX induces oxidative stress, DNA damage, lipid peroxidation, calcium imbalance, and activation of p53-dependent pathways, ultimately leading to apoptosis (Bedoschi et al, 2016; Nguyen et al, 2025; Markowska et al, 2024; Guo et al, 2021; Rad et al, 2021). DOX also damages granulosa cells, promotes follicular atresia, triggers premature activation of primordial follicles, and disrupts the hypothalamic–pituitary–gonadal axis by reducing levels of estradiol, progesterone, FSH, and LH hormones (Markowska et al, 2024; Rad et al, 2021). Doxorubicin treatment induces apoptosis in ovarian tissue by upregulating pro-apoptotic gene Bax and downregulating the anti-apoptotic gene Bcl-2, leading to follicular cell death, ovarian dysfunction and impaired steroidogenesis (Cai et al, 2019; Saleh et al, 2020; Zhang et al, 2017). DOX induces significant histopathological alterations in the ovary including follicular atresia, which is characterized with a marked reduction in the number of primordial and secondary follicles (Gao et al, 2023, Nishi et al, 2018). DOX therapy induces vascular damage and fibrosis of the ovarian stroma, resulting in the onset of premature ovarian failure (POF) (Soleimani et al, 2011).

Given the toxic effects of DOX on the ovaries, there is increasing interest in identifying protective agents that can mitigate chemotherapy-induced gonadotoxicity. Itaconate, an immunometabolite produced by macrophages through ACOD1 enzyme activation in response to inflammatory stimuli such as LPS, has demonstrated anti-inflammatory and antioxidant properties in various pathological conditions (Hosseinkhani et al, 2024; Khadem et al, 2022; Azari et al, 2024). Dimethyl itaconate (DMI) and 4-octyl itaconate (4-OI) are the most studied cell permeable derivatives of itaconic acid. These derivatives exert anti-inflammatory effects primarily through activation of the Nrf2 pathway and inhibition of the Keap1–Nrf2 complex (Ferreira et al, 2023). They also suppress key pro-inflammatory pathways, including NF-κB and NLRP3 inflammasome activation (Azari et al, 2024). In addition, they reduce reactive oxygen species (ROS) production and upregulate antioxidant enzymes such as HO-1 and NQO1. By modulating cellular metabolism and enhancing immunity, itaconate derivatives help maintain redox balance and protect against inflammation-induced tissue damage (Zhan et al, 2022). Limited data are available regarding the role of itaconic acid in regulating ovarian function. Recently, it was found that in bovine granulosa cells, DMI suppresses LPS-induced inflammation by downregulating NLRP3 and TLR4 pathways and inhibiting NF-κB and JNK signaling pathways, thereby reducing the expression of pro-inflammatory cytokines (Tabandeh et al, 2022). It has been also reported that DMI alleviates ovarian dysfunction in a rat model of PCOS by reducing oxidative stress, inflammation, and insulin resistance. Recently, He et al, (2023) showed that growth hormone co-treatment in women with diminished ovarian reserve significantly altered follicular fluid metabolism. Notably, itaconic acid was elevated alongside glutathione, and its levels positively correlated with the number of oocytes retrieved. Recent evidence showed that DMI has protecting role against chemotherapy-induced toxicity in non-reproductive organs. Shan et al, (2019) demonstrated that *DMI* alleviated acute DOX-induced heart injury in mice by activating the Nrf2/HO-1 antioxidant pathway. Daneshmandi et al, (2024) found that *4-OI* protected both monocytic and

polymorphonuclear cells from DOX-induced apoptosis and mitochondrial ROS accumulation. However, no data are available about the possible protective effects of DMI against ovarian toxicity induced by chemotherapy.

Therefore, the present study aims to evaluate the protective effects of DMI against DOX-induced ovarian toxicity in a 4T1 murine model of breast cancer. Specifically, this study focuses on assessing histological changes, apoptosis-related gene expression, and alterations in sex hormone production to determine whether DMI can mitigate gonadotoxicity and preserve ovarian function during chemotherapy.

Materials and Methods

Experimental Animals

A total of 30 adult female BALB/c mice with breast cancer (average weight 20 ± 2 g) were obtained from AvinStemGene Biohealth laboratory. The animals were housed in standard cages under controlled temperature (25±2°C), relative humidity (55% ±15%), and a 12-hour light/12-hour dark cycle. Food and water were provided ad libitum using standard laboratory chow (Pars Feed, Iran). All procedures were approved by the Ethics Committee of Shahid Chamran University of Ahvaz (EE/1404.085/scu.ac.ir).

4T1 breast cancer mouse model

A total of 24 adult female BALB/c mice were used to develop the 4T1 breast cancer mouse model. 4T1 cell line was obtained from the AvinStemGene Biohealth laboratory (Iran, Ahvaz). Cells were cultured in a DMEM-HG medium (Bioidea, Iran), supplemented with 10% fetal bovine serum (FBS, Biosera, France) and 100 unit/ml penicillin/streptomycin (Bioidea, Iran). Cells were incubated at 37°C with 5% CO2 and 95% humidity for 36 h. Approximately, 100 µL of 1×10^5 4T1 cells were isolated and introduced subcutaneously at the 3rd mammary fat pad of the BALB/c mice as described earlier (Laftah et al, 2025). The appearance of tumors was checked once a week.

Experimental design

When tumors became palpable and the tumor size reached the 10 mm, tumor-bearing mice were randomly assigned to five groups (n=6 per group):

Group 1: Normal (Healthy Control): Healthy mice maintained under identical environmental and dietary conditions as the other groups.

Group 2: Cancer (Cancer Control): Mice bearing breast tumor that received no anticancer treatment during the study.

Group 3: Cancer + DOX: Tumor-bearing mice treated with DOX (5 mg/kg; once a week; IP) for four consecutive weeks (Ramezani et al, 2024).

Group 4: Cancer + DMI: Tumor-bearing mice treated with DMI (50 mg/kg; daily; IP) for four weeks (Hosseinkhani et al, 2024).

Group 5: Cancer + DOX + DMI: Tumor-bearing mice simultaneously treated with both DOX (5 mg/kg; once a week; IP) and DMI (50 mg/kg; daily; IP,) for four weeks.

Sample Collection

At the end of the experiment, the animals were anesthetized with ketamine hydrochloride (100 mg/kg) and xylazine (10 mg/kg). Blood samples were obtained via cardiac puncture. Serum samples were collected by centrifuging at *5000 × RPM for 10 min and stored at -20*°C for serum biochemical analysis. The ovaries were removed and fixed in Bouin's solution for histological evaluation. The ovary was also collected and stored at -70 °C for gene expression analysis (Figure 1).

Histological Analysis

Ovarian tissues were fixed in Bouin's solution for 72 h. After fixation, the tissues were dehydrated, embedded in paraffin, and sectioned at 5–7 µm thickness. Sections were mounted on glass slides and dried

overnight at 37°C. After deparaffinization, the sections were stained with hematoxylin and eosin (H&E) and periodic acid–Schiff (PAS). Folliculogenesis was evaluated by assessing atretic follicles, corpora lutea, and granulosa cell layers. Five sections per ovary were examined using a light microscope (Olympus PX 50 F3, Japan) Histological images were captured using a Dino-Lite digital (FDP2, Taiwan) microscope camera and analyzed with DinoCapture 2.0 software.

Hormonal assay

The serum estradiol (E2) and progesterone (P4) concentrations were determined by using ELISA Kits (Diametra, Italy) according to the manufacturer's instructions. All samples were run in one assay to avoid inter-assay variation. The limits of detection of P4 and E2 were 0.05 ng/ml and 5 pg/ml, respectively. The intra-assay coefficients of variation of both hormones were less than 10%. All assays were carried out in duplicate.

RNA extraction and cDNA synthesis

Total RNA was extracted using the Total RNA Extraction Kit (Pars Tous, Iran), following the manufacturer's instructions. The purity of RNA at 260/280 OD ratio and the RNA integrity was evaluated using an Eppendorf µCuvette G1.0 microvolume measuring cell (Eppendorf, Germany). High-purity RNA with an OD of 260/280 ratio above 1.8 was used for cDNA synthesis. The cDNA was synthesized using 1 µg of RNA by Easy™ cDNA Synthesis Kit (ParsTous, Iran) and random hexamer according to the manufacturer's instructions.

Real-Time PCR analysis

To assess the expression levels of Bax and Bcl2 genes in ovary, real-time PCR (qRT-PCR) analysis was performed. The qRT-PCR primers were designed using the Primer3 software version 4.1.1 based on the sequences ofBax, Bcl2 and GAPDH genes available in NCBI Genebank (Table 1). The SYBR® Green Real Time PCR Master mix (ParsTous, Iran) was used to perform qRT-PCR on the Lava96T^{M} Real-Time PCR detection System (DaanGene, Co, Ldt, China). The thermal cycling conditions were as follows: initial denaturation at 94°C for 5 min; 45 cycles of: 94°C for 15 s and 60°C for 25 s. Two control reactions including a negative control without cDNA and a control containing RNA instead of DNA were considered. The relative expression of the genes compared to the calibrator gene was analyzed using the comparative $2^{-\Delta\Delta Ct}$ method. Evaluation of the amplification efficiency of the target genes compared to the reference gene (GAPDH) was done by preparing different dilutions of cDNA and drawing the efficiency graph as described previously (Tabandeh et al, 2022).

Table 1: Characteristics of primers that used in the current study

Gene	Forward Primer (5'→3')	Reverse Primer (5'→3')	Product Size (bp)	Accession No.
GAPDH	AGCCTTCTCCATGGTGGTGA	TGAAGTCGCAGGAGACAACC	116	NM_001289726.2
BAX	TGGAGCTGCAGAGGATGATT	CAGTTGAAGTTGCCATCAGCA	110	NM_017059.2
BCL-2	ATGGAGCTGCAGAGGATGAT	AGTTGAAGTTGCCATCAGCA	100	NM_007527.4

Statistical analysis

Statistical analysis was performed using GraphPad Prism software version 10 (Graph Pad Software, Inc., San Diego, CA). For evaluating the statistical significance of differences between groups, one-way analysis of variance (ANOVA) with Tukey's post hoc test was performed. Data are expressed as mean ± standard deviation (SD). Statistically significance difference between different experimental groups was represented as follows: #, *p< 0.05, ##, **p< 0.01, ###, *** p< 0.001, #### **** p<0.0001.

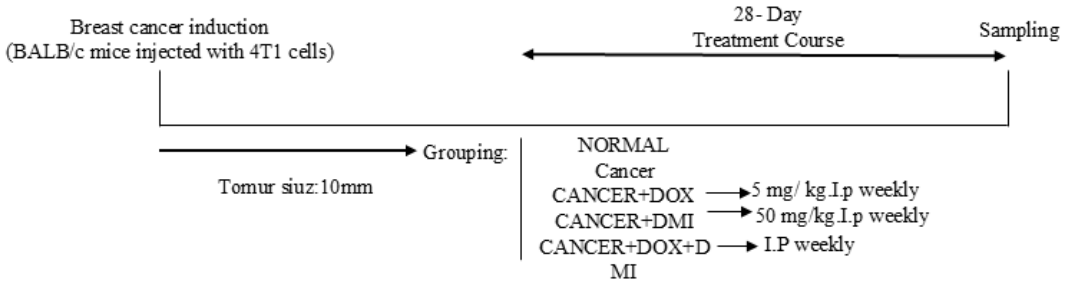

Figure 1: Overview of 5-week experimental protocol.

Results

Effects of DMI on histological alterations in the ovaries of DOX treated mice bearing breast cancer

In the healthy control (normal) group, the ovaries showed normal histological architecture. This included an intact stromal matrix, a regular surface epithelium, and follicles at various developmental stages such as primordial, primary, secondary, preantral, antral, and atretic follicles characterized by signs of apoptosis and pyknosis. The corpus luteum structures, normal blood vessels and vascular networks, and occasionally follicles containing two oocytes were also observed (Figure 2-A). In the cancer control group, the ovarian stroma showed increased cellular density compared to the normal group. The surface epithelium appeared thickened in areas containing developing primordial and primary follicles, with epithelial cells showing enlargement and notable morphological alterations. A prominent vascular network composed of dilated and congested blood vessels was observed in the central region of the ovary and beneath the surface epithelium. Numerous atretic follicles, mainly at the secondary to preantral stages, were identified. These atretic follicles were often elongated in shape. The corpus luteum was either rarely seen or entirely absent (Figure 2-B). In the cancer group treated with DOX (Cancer + DOX group), the ovarian stroma displayed a lower cellular density compared to the cancer control group. A broad vascular network remained present in the central ovarian region and beneath the surface epithelium, although it was less prominent than in the cancer control group. Follicles were generally smaller in size compared to those in the cancer control group, and the surface epithelium remained thickened. Various types of atretic follicles were observed, and their numbers were higher than in the cancer control group. No corpus luteum structures were detected in this group. Notably, the number of primordial and primary follicles was considerably higher than in both the healthy and cancer control groups (Figure 2-C). In the cancer mice group treated with DMI (Cancer + DMI group), the ovarian stroma showed a lower cellular density compared to the cancer control group. A vascular network was observed within the stromal region of the ovarian cortex and beneath the surface epithelium. The number of atretic follicles in this group was lower than in the group treated with DOX. These atretic follicles included various follicular types and mainly involved isolated granulosa cells, with the zona pellucida being less affected. The number of primordial and primary follicles was higher in this group than in the healthy control, cancer control, and Cancer + DOX + DMI groups, but lower than in the Cancer + DOX group. Secondary follicles in this group typically appeared round and spherical. The ovarian surface epithelium was thinner compared to that in the DOX-treated group. No corpus

luteum was observed (Figure 2-D). In the cancer + DOX + DMI group, the cellular density of the ovarian stroma was lower than that in the Cancer + DOX group. The corpus luteum was either rarely observed or completely absent. A vascular network was present in the central region of the ovary, but it was less extensive compared to the Cancer + DOX group. Although there was no marked increase in the thickness of the surface epithelium, the epithelial cells appeared larger than those observed in the Cancer + DOX group. The number of atretic follicles in this group was lower than in the group treated with DOX (Figure 2-E).

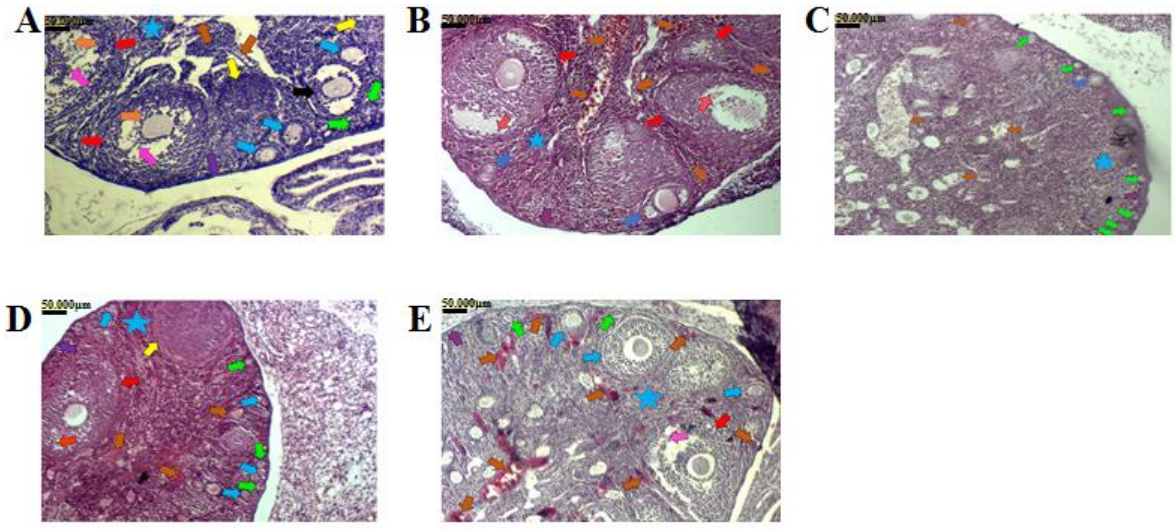

Figure 2: Sections of ovarian tissue from different experimental groups (A) Healthy control, (B) Cancer control, (C) Cancer + DOX, (D) Cancer + DMI, (E) Cancer + DOX + DMI (H&E, 10X). Yellow arrowhead: corpus luteum, green arrow: primary follicle, blue arrow: secondary follicle, black arrow: antral follicle, red arrow: atretic follicle, purple arrow: ovarian surface epithelium, brown arrow: blood vessels, orange arrow: pyknotic nucleus, pink arrow: apoptotic bodies within atretic follicles, blue asterisk indicates the stromal matrix.

Evaluation of Zona Pellucida Uniformity

To evaluate the structural integrity of the zona pellucida, PAS staining was conducted on ovarian sections from all experimental groups. In the healthy control group, the zona pellucida showed its structural continuity and showed minimal signs of atresia (Figure 3-A). In contrast, the cancer control group exhibited disrupted zona pellucida morphology in many atretic follicles, characterized by irregular thickness. In certain regions, the zona pellucida appeared markedly thinned, detached, and freely floating within the antrum, displaying an undulating pattern (Figure 3-B). In DOX group, the zona pellucida exhibited irregular thickness and a wavy morphology. Areas of disrupted continuity and compromised structural integrity were more frequently observed compared to the cancer control group. These alterations were notably more severe than those in the cancer control group (Figure 3-C). In the Cancer + DMI group, the zona pellucida showed a pattern similar to the Cancer + DOX group, characterized by uneven thickness, a wavy appearance, and increased fragmentation and discontinuities compared to the cancer control group (Figure 3-D). In the Cancer + DOX + DMI group, the zona pellucida thickness in many atretic follicles was more uniform compared to the Cancer + DOX group (Figure 3-E).

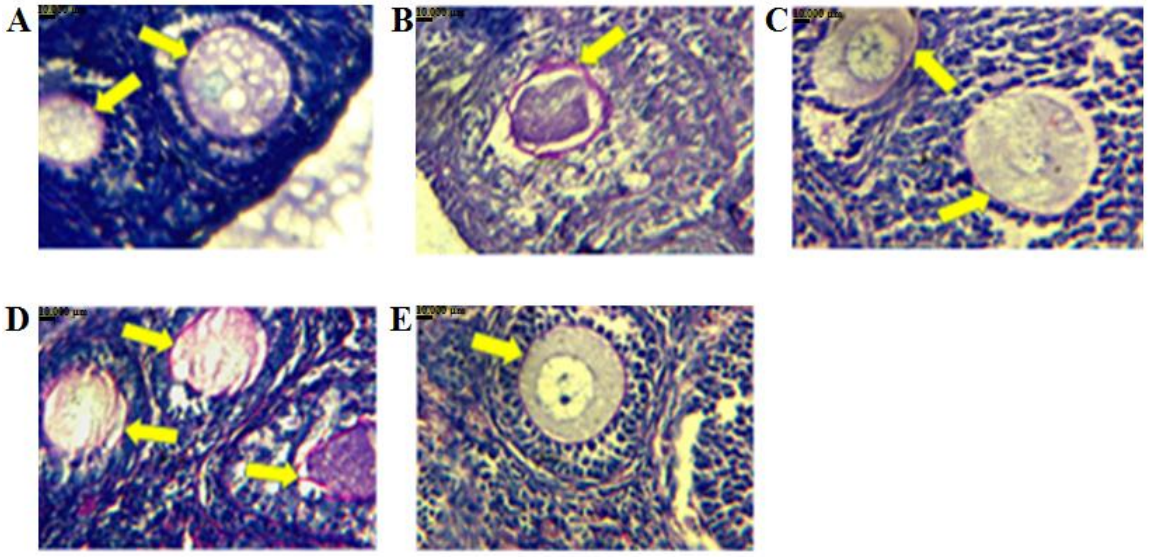

Figure 3: Ovarian tissue sections examined from five experimental groups, focusing on the zona pellucid. Groups: (A) Healthy control, (B) Cancer control, (C) Cancer + DOX, (D) Cancer + DMI, (E) Cancer + DOX + DMI (PAS, 40X). Yellow arrow: zona pellucid.

Effect of DMI on serum estradiol and progesterone concentrations in DOX-treated mice bearing breast cancer

Serum estradiol level was significantly reduced in the cancer group compared to the normal (control) group ($P<0.01$). This reduction was even more pronounced in the cancer + DOX group, which showed a further significant decrease compared to the cancer group ($P<0.01$). Treatment of cancer-bearing mice with DMI alone had no significant effect on serum estradiol concentration when compared to untreated cancer mice ($P>0.05$). However, in DOX-treated mice, co-administration of DMI significantly elevated serum estradiol level compared to those receiving DOX alone ($P<0.05$) (Figure 4-A). Serum progesterone level was significantly reduced in the cancer group compared to the normal control group ($P<0.0001$). The Cancer + DOX group exhibited a greater decrease in serum progesterone level compared to the cancer group ($P<0.0001$). Treatment of cancer-bearing mice with DMI had no significant effect on serum progesterone concentration compared to untreated cancer mice ($P>0.05$). However, in DOX-treated mice, DMI significantly increased serum progesterone level compared to untreated animals ($P<0.01$) (Figure 4-B).

Effect of DMI on ovarian expression of apoptosis related genes in DOX-treated mice bearing breast cancer

There was no significant difference in the relative expression level of the Bax gene between the cancer group and the normal group ($P>0.05$). DMI administraion in cancer mice had no significant effect on Bax gene expression compared to untreated mice. The Bax expression level was increased in the cancer + DOX group compared to the cancer group ($P<0.0001$). DMI could reduce the expression of Bax gene in ovary of DOX-treated mice compared to the un treated mice ($P<0.01$) (Figure 5-A). There was a significant decrease in the relative expression level of the Bcl2 gene in the cancer group compared to the normal group ($P<0.01$). Administration of DMI in cancer-bearing mice significantly increased Bcl2 gene expression compared to untreated cancer mice ($P<0.05$). However, BCL2 expression was reduced in the cancer + DOX group compared to the cancer group ($P<0.01$). DMI was able to increase Bcl2 gene expression in the ovaries of DOX-treated mice compared to those treated with DOX alone ($P<0.05$) (Figure 5-B).

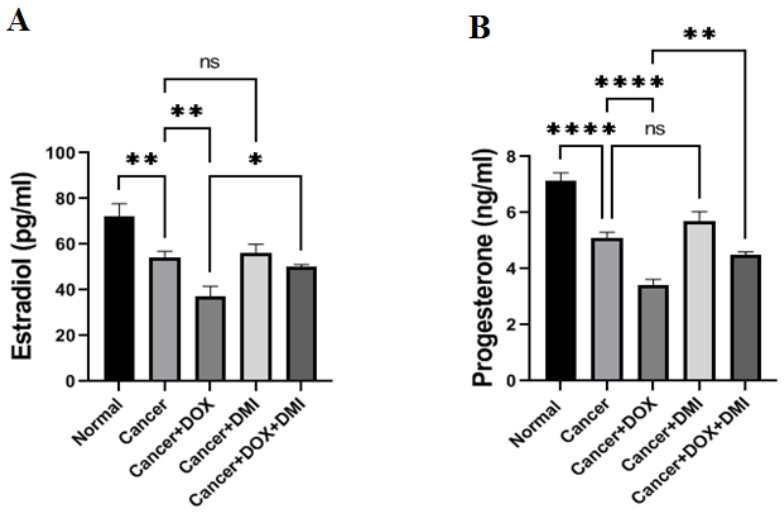

Figure 4: Serum concentrations of estradiol (A) and progesterone (B) in healthy mice (normal), 4T1 breast cancer-bearing mice (cancer), cancer-bearing mice treated with DOX (cancer + DOX), cancer-bearing mice treated with DMI (cancer + DMI), and cancer-bearing mice treated with both DOX and DMI (cancer + DOX + DMI). Data are presented as mean ± SD (n = 6 per group). Statistical significance is indicated as follows: ns, not significant; *p < 0.05; **p < 0.01; ****p < 0.0001

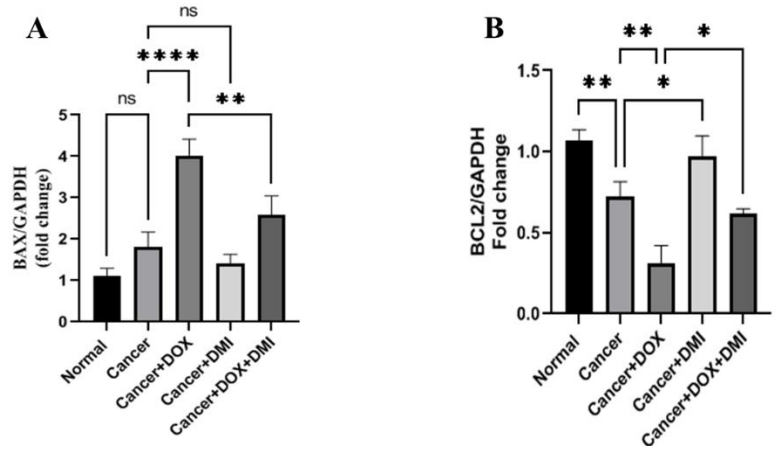

Figure 5: Ovarian expression levels of Bax (A) and Bcl2 (B) genes in different experimental groups. healthy mice (normal), 4T1 breast cancer mice (cancer), breast cancer mice treated with DOX (cancer + DOX), breast cancer mice treated with DMI (cancer +DMI), and breast cancer mice treated with both DOX and DMI (cancer +DOX + DMI). The GAPDH was used as a housekeeping gene. Relative quantification was performed according to the comparative $2^{-\Delta\Delta Ct}$ method. Data represent mean ± SD for 6 animals in each group. Statistical significance is denoted as follows: *p < 0.05; **p < 0.01; ***p < 0.001; ns indicates not significant.

Discussion

DOX is one of the most common drugs widely used in breast cancer treatment. However, although effective against tumor, it can adversely affect ovarian function and fertility in women of reproductive age. Damage to growing follicles, increased apoptosis of granulosa cells, and disruptions in sex hormone production are well-documented side effects of DOX. Consequently, the combination of protective agents with DOX therapy has emerged as a promising strategy to mitigate

DOX-induced toxicity and preserve fertility in patients undergoing treatment. DMI, a metabolite derived from macrophage metabolic pathways, is considered a potential cytoprotective agent because it can activate the Nrf2 pathway and reduce oxidative stress and inflammation. This study aimed to explore the effects of DMI on apoptosis, folliculogenesis, and serum sex hormone production in a mouse model of breast cancer receiving DOX treatment. The results provide new insights into protecting the ovaries during cancer treatment through the use of DMI.

Results indicated that mice bearing breast tumors had reduced serum estradiol and progesterone levels, and DOX treatment further exacerbated this reduction. Additionally, tumor-bearing mice exhibited increased expression of the pro-apoptotic gene Bax and decreased expression of the anti-apoptotic gene Bcl-2, effects that were further potentiated by DOX treatment. Histological evaluations revealed impaired normal folliculogenesis in the ovaries of cancer-bearing mice as well as in those treated with DOX. In the ovary of cancer control group, many degenerating atretic follicles, especially at early developmental stages, were observed, and corpus luteum formation was minimal or absent. Treatment with DOX reduced stromal cellular density and vascular prominence but increased the number of early-stage (primordial and primary) follicles. These results suggest that DOX treatment alters ovarian structure by reducing cellular density and vascularization while preserving or even increasing the early follicle pool, potentially impacting ovarian function differently than untreated cancer. In the untreated cancer group, reduced serum estradiol and progesterone closely corresponded with increased follicular atresia and decreased secondary and antral follicles, highlighting the dependency of folliculogenesis on steroid hormones. Doxorubicin exacerbated these effects through granulosa cell apoptosis (Bax↑, Bcl-2↓) and loss of growing follicles, resulting in impaired steroidogenesis. In contrast, DMI treatment, alone or combined with DOX, preserved granulosa cell survival, maintained secondary follicles, and reduced atresia, thereby supporting follicular growth and steroid hormone production. Changes in steroid hormone levels are directly associated with folliculogenesis in the ovary; reduced estradiol and progesterone correlate with increased follicular atresia and loss of growing follicles, whereas preservation of granulosa cell survival supports follicle maintenance and steroid hormone production (Chauvin et al., 2022). Although most studies on cancer-related gonadotoxicity have focused on chemotherapy, our results indicated that tumor itself can disrupt reproductive function. The previous studies have indicated that systemic tumors may exert distant effects on the ovary through inflammatory cytokines, metabolic modukators, or hormonal feedback dysregulation. Supporting it, studies in tumor-bearing rodents have shown alterations in the hypothalamic-pituitary-gonadal axis, which can impair gonadotropin release and disrupt folliculogenesis. Inflammation and oxidative stress induced by tumor burden may also contribute to granulosa cell dysfunction and apoptosis. Wang et al (2017) reported that tumor-bearing mice showed loss of both primordial and growing follicles, alongside abnormal steroid hormone levels and elevated ROS in ovarian tissue. They linked tumor-induced ovarian damage to mitochondrial dysfunction in oocytes and granulosa cells via the PI3K–Akt–mTOR pathway (Wu et al, 2023). These mechanisms align with our observed increase in Bax expression and reduction in Bcl-2, markers of mitochondrial-mediated apoptosis in ovary of mice bearing cancer showed impaired follicular development. Further, supporting this interpretation, inflammation-associated

cytokines such as IL-6 and TNF-α—known to be elevated in tumor-bearing mice and breast cancer patients—can directly inhibit granulosa cell steroidogenesis and promote apoptotic signaling (Ojo et al, 2023). Furthermore, breast cancer is known to be hormonally responsive, and its metabolic activity may affect systemic estrogen levels or feedback regulation on the ovary. Reduced levels of E2 and P4 in our cancer-induced mice are consistent with findings from stress or toxin-induced ovarian dysfunction models, where hormonal imbalances are typically accompanied by granulosa cell apoptosis and follicle depletion. Moreover, ovarian cachexia models showed that cancer-induced dysregulation of ovarian hormones often precedes overt weight loss and systemic symptoms (Guo et al, 2024). This highlights that tumor presence disrupts the hypothalamic–pituitary–gonadal axis early on, consistent with our observations of reduced E_2/P_4 and declining follicle counts (Hetzler et al, 2017). Taken together, our data support the hypothesis that breast tumor presence alone is sufficient to induce ovarian damage, potentially through endocrine, inflammatory, and apoptotic pathways. This underlines the importance of considering tumor-related effects on fertility even before the initiation of chemotherapy and suggests a need for early fertility assessment and intervention in cancer patients.

In accordance with our findings Ben-Aharon et al, (2010) indicated that DOX treatment caused a significant reduction in ovarian weight, increasing follicular atresia, particularly secondary and antral follicles and a marked depletion of the ovarian follicle reserve and granulosa cell apoptosis one month after treatment with DOX. Additionally, serum estradiol levels were significantly decreased following DOX exposure, reflecting impaired steroidogenesis. At the molecular level, DOX induced upregulation of pro-apoptotic genes such as Bax and downregulation of anti-apoptotic genes like Bcl-2, alongside increased caspase-3 activation, confirming activation of the apoptotic pathway. Wang et al, (2017) showed that DOX depletes the ovarian reserve through a dual mechanism involving both direct oocyte apoptosis and indirect overactivation of primordial follicles. Their study demonstrated that DOX causes DNA double-strand breaks, particularly in granulosa cells and oocytes of growing follicles, triggering apoptosis via the TAp63α–caspase-3 pathway. These findings collectively demonstrate that DOX induces ovarian toxicity by promoting granulosa cell apoptosis, follicular atresia, and hormonal disruption, thereby compromising ovarian reserve and function.

Researchers showed that administration of DMI significantly reversed ovarian pathological and molecular changes induced by DOX therapy. DMI treatment restored the number of growing follicles, improved the morphology of ovarian tissue, and supported the reappearance of corpus luteum structures. In addition, DMI improved the serum levels of E_2 and P_4 and balanced the expression of Bax and Bcl-2, indicating a reduction in DOX and tumor-induced apoptotic signaling. These results suggest that DMI exerts a protective effect on the ovary under conditions of oxidative and apoptotic stress associated with cancer and chemotherapy.

The observed variations in serum E2 and P4 levels across the groups suggest differential impacts on ovarian follicular development and luteal function. Estradiol production during the follicular phase primarily depends on the activity of growing antral follicles, while progesterone secretion during the luteal phase is contingent upon the presence of a functional corpus luteum. In the cancer and cancer + DOX groups, reductions in both E2 and P4 levels reflect disrupted folliculogenesis, increased follicular atresia, and regression or loss of the corpus luteum. These changes can be attributed to the combined effects of

tumor-induced systemic stress and the cytotoxicity of DOX, both of which are known to induce oxidative damage, impaired granulosa and luteal cell function, and accelerate ovarian follicle depletion (Markowska et al , 2024; Rad et al, 2021; Guo et al, 2024). In contrast, the restoration of E2 and P4 levels in the cancer + DOX + DMI and cancer + DMI groups suggests that DMI may exert a protective role in ovarian physiology. DMI's antioxidant and anti-inflammatory properties may contribute to an improved ovarian microenvironment, preserving granulosa and luteal cell viability, sustaining steroidogenic enzymes activity, and facilitating the development of a functional corpus luteum. This can support both estradiol biosynthesis and progesterone production. Taken together, the recovery of serum estradiol and progesterone levels in the DMI-treated group underscores DMI's potential to mitigate chemotherapy- and cancer-induced ovarian dysfunction. By enhancing follicular survival and preserving luteal activity, DMI may contribute to the maintenance of endocrine function and reproductive health under conditions of oncogenic and chemotherapeutic stress. These findings highlight the therapeutic potential of DMI in protecting ovarian integrity and function during cancer treatment.

Several mechanisms may be related to improvement of ovarian dysfunctions in DOX-treated mice following DMI treatment. One of the primary mechanisms by which DMI exerts its protective effect against ovarian dysfunctions is via activation of the Nrf2 (nuclear factor erythroid 2–related factor 2) pathway. DMI alkylates specific cysteine residues on KEAP1, the cytoplasmic repressor of Nrf2, thereby disrupting KEAP1-mediated degradation of Nrf2. Stabilized Nrf2 translocates to the nucleus, where it binds to antioxidant response elements (AREs) in the promoters of target genes involved in redox homeostasis, including HO-1, NQO1, and glutathione biosynthesis enzymes (Mills et al, 2018). This leads to upregulation of cellular antioxidant defenses and a corresponding reduction in ROS. In addition to its antioxidant effects, DMI also exerts anti-inflammatory activity through suppression of the NF-κB signaling pathway. It interferes with the phosphorylation and degradation of IκBα, thereby preventing nuclear translocation of the p65/p50 NF-κB complex. Furthermore, DMI may directly alkylate cysteine residues on upstream kinases such as IKKβ, leading to broad inhibition of NF-κB–dependent transcription of proinflammatory cytokines, including TNF-α, IL-1β, and IL-6 (Williams et al, 2018; O'Neill et al, 2019). Another important target of DMI is succinate dehydrogenase (SDH), a key mitochondrial enzyme whose inhibition reduces succinate oxidation and downstream ROS production, further contributing to redox balance and inhibition of HIF-1α–mediated proinflammatory gene expression. Collectively, these mechanisms demonstrate how DMI modulates both inflammatory and oxidative stress responses, highlighting its potential therapeutic application in protecting granulosa cells and ovarian tissue under pathological conditions such as DOX-induced gonadotoxicity.

To support this hypothesis, DMI has been shown to restore steroidogenesis and improve granulosa cell viability under inflammatory conditions. In a recent study, Tabandeh et al, (2022) reported that DMI significantly improved E2 and P4 production in lipopolysaccharide treated bovine ovarian granulosa cells, a well-established model of inflammation-induced ovarian dysfunction. LPS exposure activated key inflammatory signaling pathways, including TLR4/NF-κB, NLRP3 inflammasome, and JNK, leading to impaired cell viability, suppressed steroidogenesis, and increased production of proinflammatory cytokines such as IL-1β and TNF-α. Treatment with DMI

effectively countered these effects by downregulating the expression and activation of TLR4, NF-κB, NLRP3, and phosphorylated JNK. This was accompanied by a reduction in inflammatory cytokine release and restoration of steroidogenic function, suggesting that DMI exerts its protective effects by modulating inflammatory signaling and preserving granulosa cell function. Recently, Hosseinkhani et al (2024), indicated that DMI ameliorated ovarian dysfunction in a rat model of testosterone-induced PCOS. Their findings demonstrated that DMI exhibited strong anti-inflammatory effects by decreasing ovarian levels of pro-inflammatory cytokines, including TNF-α and IL-1β. It also reduced oxidative stress, as evidenced by a lower ovarian oxidative stress index (OSI). Histological evaluations revealed that DMI improved folliculogenesis, decreased the number of cystic follicles, and restored normal ovarian tissue architecture. Additionally, it enhanced ovarian steroidogenic function. Zhou et al (2020), also showed that itaconic acid, through its endogenous enzyme IRG1, exerted a protective effect against endoplasmic reticulum (ER) stress–induced necroptosis in bovine granulosa cells. They demonstrated that itaconic acid attenuated tunicamycin-induced ER stress by inhibiting the PERK–ATF4 signaling pathway and reducing acetylcholinesterase (AChE) expression, which in turn suppressed necroptosis and preserved cell viability and ultrastructure. These findings highlight a novel role of itaconate in maintaining granulosa cell function under stress conditions (Yang et al, 2025).

This study demonstrated that breast tumor induction and DOX chemotherapy significantly disrupt ovarian hormone levels, gene expression related to apoptosis, and ovarian follicular development. DOX treatments further exacerbate tumor-induced ovarian damage by altering ovarian structure, reducing cellular density and vascularization, and increasing follicular atresia. Importantly, DMI administration effectively mitigates these detrimental effects by restoring normal ovarian morphology, hormone balance, and apoptotic gene expression. These findings suggest that DMI has a protective role against cancer and chemotherapy-induced ovarian dysfunction, highlighting its potential as a therapeutic agent to preserve ovarian health during breast cancer treatment.

Ethical statement

All protocols and procedures were in compliance with international guidelines for care and use of laboratory animals, and they were approved by Shahid Chamran University of Ahvaz (SCU.VB1404.085/scu.ac.ir).

Acknowledgment

The authors would like to appreciate the Research Council of Shahid Chamran University of Ahvaz for funding this study.

Conflict of interest

The authors declare that they have no known competing financial interests or personal relationships that could have appeared to influence the work reported in this paper.

Funding

This study was supported by a grant (no SCU.VB1404.158) from the Shahid Chamran University of Ahvaz, Iran.

References

Azari, N., Rezaee, M., Dayer, D., & Tabandeh, M. R. (2024). Dimethyl itaconate modulates neuroprotective effect on primary rat astrocytes under inflammatory condition by regulating the expression of neurotrophic factors and TrkA/B-P75 receptors. *Neurological Research*, *46*(12), 1137–1148.

Bedoschi, G., Navarro, P. A., & Oktay, K. (2016). Chemotherapy-induced damage to ovary: Mechanisms and clinical impact. *Future Oncology*, *12*(20), 2333–2344.

Ben-Aharon, I., Bar-Joseph, H., Tzarfaty, G., Kuchinsky, L., Rizel, S., Stemmer, S. M., & Shalgi, R. (2010). Doxorubicin-induced ovarian toxicity. *Reproductive Biology and Endocrinology*, *8*, 1–7.

Cai, G., Si, M., Li, X., Zou, H., Gu, J., Yuan, Y., ... & Bian, J. (2019). Zearalenone induces apoptosis of rat Sertoli cells through Fas-Fas ligand and mitochondrial pathway. *Environmental Toxicology*, *34*(4), 424–433.

Chauvin, S., Cohen-Tannoudji, J., & Guigon, C. J. (2022). Estradiol signaling at the heart of folliculogenesis: Its potential deregulation in human ovarian pathologies. *International Journal of Molecular Sciences*, *23*(1), 512.

Daneshmandi, S., Choi, J. E., Yan, Q., MacDonald, C. R., Pandey, M., Goruganthu, M., ... & Mohammadpour, H. (2024). Myeloid-derived suppressor cell mitochondrial fitness governs chemotherapeutic efficacy in hematologic malignancies. *Nature Communications*, *15*(1), 2803.

Ferreira, A. V., Kostidis, S., Groh, L. A., Koeken, V. A., Bruno, M., Baydemir, I., ... & Netea, M. G. (2023). Dimethyl itaconate induces long-term innate immune responses and confers protection against infection. *Cell Reports*, *42*(6), Article 112558.

Gao, Y., Wu, T., Tang, X., Wen, J., Zhang, Y., Zhang, J., & Wang, S. (2023). Increased cellular senescence in doxorubicin-induced murine ovarian injury: Effect of senolytics. *Geroscience*, *45*(3), 1775–1790.

Guo, S., Quan, S., & Zou, S. (2021). Roles of the notch signaling pathway in ovarian functioning. *Reproductive Sciences*, *28*(10), 2770–2778.

Guo, Y., Xue, L., Tang, W., Xiong, J., Chen, D., Dai, Y., ... & Wang, S. (2024). Ovarian microenvironment: Challenges and opportunities in protecting against chemotherapy-associated ovarian damage. *Human Reproduction Update*, *30*(5), 614–647.

He, F., Wang, F., Yang, Y., Yuan, Z., Sun, C., Zou, H., ... & Han, T. L. (2023). The effect of growth hormone on the metabolome of follicular fluid in patients with diminished ovarian reserve. *Reproductive Biology and Endocrinology*, *21*(1), 21.

Hetzler, K. L., Hardee, J. P., LaVoie, H. A., Murphy, E. A., & Carson, J. A. (2017). Ovarian function's role during cancer cachexia progression in the female mouse. *American Journal of Physiology-Endocrinology and Metabolism*, *312*(5), E447–E459.

Hosseinkhani, F., Hosseinifar, S., & Tabandeh, M. R. (2024). Dimethyl itaconate mitigates histological distortions, inflammation, and oxidative stress in the rat model of polycystic ovary syndrome. *The Journal of Steroid Biochemistry and Molecular Biology*, *243*, Article 106546.

Khadem, M. D., Tabandeh, M. R., Haschemi, A., Kheirollah, A., & Shahriari, A. (2022). Dimethyl itaconate reprograms neurotoxic to neuroprotective primary astrocytes through the regulation of NLRP3 inflammasome and NRF2/HO-1 pathways. *Molecular and Cellular Neuroscience*, *122*, Article 103758.

Laftah, A. H., Alhelfi, N., Al Salait, S. K., Altemimi, A. B., Tabandeh, M. R., Tsakali, E., ... & Abedelmaksoud, T. G. (2025). Mitigation of doxorubicin-induced liver toxicity in mice breast cancer model by green tea and Moringa oleifera combination: Targeting apoptosis, inflammation, and oxidative stress. *Journal of Functional Foods*, *124*, Article 106626.

Markowska, A., Antoszczak, M., Markowska, J., & Huczyński, A. (2024). Gynotoxic effects of chemotherapy and potential protective mechanisms. *Cancers*, *16*(12), 2288.

Mills, E. L., Ryan, D. G., Prag, H. A., Dikovskaya, D., Menon, D., Zaslona, Z., ... & O'Neill, L. A. (2018). Itaconate is an anti-inflammatory metabolite that activates Nrf2 via alkylation of KEAP1. *Nature*, *556*(7699), 113–117.

Nguyen, N. M. P., Chang, E. M., Chauvin, M., Sicher, N., Kashiwagi, A., Nagykery, N., ... & Oktay, K. (2025). AMH protects the ovary from doxorubicin by regulating cell fate and the response to DNA damage. *Proceedings of the National Academy of Sciences*, *122*(5), e2414734122.

Nishi, K., Gunasekaran, V. P., Arunachalam, J., & Ganeshan, M. (2018). Doxorubicin-induced female reproductive toxicity: An assessment of ovarian follicular apoptosis, cyclicity and reproductive tissue histology in Wistar rats. *Drug and Chemical Toxicology*, *41*(1), 72–81.

Ojo, O. A., Nwafor-Ezeh, P. I., Rotimi, D. E., Iyobhebhe, M., Ogunlakin, A. D., & Ojo, A. B. (2023). Apoptosis, inflammation, and oxidative stress in infertility: A mini review. *Toxicology Reports*, *10*, 448–462.

O'Neill, L. A., & Artyomov, M. N. (2019). Itaconate: The poster child of metabolic reprogramming in macrophage function. *Nature Reviews Immunology*, *19*(5), 273–281.

Rad, P., Safari, F., Mohammadi, J., & Delaviz, H. (2021). Preserved ovarian function following toxicity with doxorubicin in rats: Protective effect of nasturtium officinale extract. *Iranian Journal of Toxicology*, *15*(1), 57–64.

Ramezani-Aliakbari, K., Jalali, S. A., Alinejad, M., Jeddi-Tehrani, M., & Shabani, M. (2024). 5-Fluorouracil effectively depletes tumor induced myeloid derived suppressor cells in 4T1 mammary carcinoma model. *Avicenna Journal of Medical Biotechnology*, *16*(4), 244–250.

Saleh, D., Abdelbaset, M., Hassan, A., Sharaf, O., Mahmoud, S., & Hegazy, R. (2020). Omega-3 fatty acids ameliorate doxorubicin-induced cardiorenal toxicity: In-vivo regulation of oxidative stress, apoptosis and renal Nox4, and in-vitro preservation of the cytotoxic efficacy. *PLoS ONE*, *15*(11), e0242175.

Shan, Q., Li, X., Zheng, M., Lin, X., Lu, G., Su, D., & Lu, X. (2019). Protective effects of dimethyl itaconate in mice acute cardiotoxicity induced by doxorubicin. *Biochemical and Biophysical Research Communications*, *517*(3), 538–544.

Soleimani, R., Heytens, E., Darzynkiewicz, Z., & Oktay, K. (2011). Mechanisms of chemotherapy-induced human ovarian aging: Double strand DNA breaks and microvascular compromise. *Aging (Albany NY)*, *3*(8), 782–793.

Tabandeh, M. R., Jozaie, S., Ghotbedin, Z., & Gorani, S. (2022). Dimethyl itaconic acid improves viability and steroidogenesis and suppresses cytokine production in LPS-treated bovine ovarian granulosa cells by regulating TLR4/nfkβ, NLRP3, JNK signaling pathways. *Research in Veterinary Science*, *152*, 89–98.

Wang, L., Wang, Y., Wang, Z., Qi, Y., Zong, B., Liu, M., ... & Ma, Y. (2018). Growth differentiation factor 11 ameliorates experimental colitis by inhibiting NLRP3 inflammasome activation. *American Journal of Physiology-Gastrointestinal and Liver Physiology*, *315*(6), G909–G920.

Williams, N. C., & O'Neill, L. A. (2018). A role for the Krebs cycle intermediate citrate in metabolic reprogramming in innate immunity and inflammation. *Frontiers in Immunology*, *9*, 141.

Wu, Y., Huang, J., Chen, H., Tao, H., He, Y., Yang, G., ... & Li, P. (2023). Tumor-derived oxidative stress triggers ovarian follicle loss in breast cancer. *The American Journal of Pathology*, *193*(5), 608–623.

Yang, X., Chen, Y., Wang, X., Xu, G., Wang, H., Shu, X., ... & Lu, W. (2025). Ameliorative effect of itaconic acid/IRG1 against endoplasmic reticulum stress-induced necroptosis in granulosa cells via PERK-ATF4-AChE pathway in bovine. *Cells*, *14*(6), 419.

Yildiz, S., Bildik, G., Benlioglu, C., Turan, V., Dilege, E., Ozel, M., ... & Oktay, K. (2023). Breast cancer treatment and ovarian function. *Reproductive BioMedicine Online*, *46*(2), 313–331.

Zhan, Z., Wang, Z., Bao, Y., Liu, W., & Hong, L. (2022). OI inhibits development of ovarian cancer by blocking crosstalk between cancer cells and macrophages via HIF-1α pathway. *Biochemical and Biophysical Research Communications*, *606*, 142–148.

Zhang, T., He, W. H., Feng, L. L., & Huang, H. G. (2017). Effect of doxorubicin-induced ovarian toxicity on mouse ovarian granulosa cells. *Regulatory Toxicology and Pharmacology*, *86*, 1–10.

Zhou, S., Xi, Y., Chen, Y., Zhang, Z., Wu, C., Yan, W., ... & Wang, S. (2020). Ovarian dysfunction induced by chronic whole-body PM2.5 exposures. *Small*, *16*(33), 2000845.

Received: 29.10.2025
Accepted: 16.02.2026

DOI: 10.22055/ivj.2026.556170.2862

تأثیر دی‌متیل‌ایتاکونات بر کاهش تغییرات بافتی و آپوپتوز تخمدان و بهبود تولید هورمون‌های جنسی در مدل تجربی سرطان پستان موش تحت درمان با دوکسوروبیسین

اعظم اسدسفتجانی[۱]، شیما حسینی‌فر[۲*] و محمدرضا تابنده[۳]

[۱] دانشجوی دکتری تخصصی بافت‌شناسی، دانشکده دامپزشکی، دانشگاه شهید چمران اهواز، اهواز، ایران
[۲] دانشیار گروه علوم پایه، دانشکده دامپزشکی، دانشگاه شهید چمران اهواز، اهواز، ایران
[۳] استاد گروه علوم پایه، دانشکده دامپزشکی، دانشگاه شهید چمران اهواز، اهواز، ایران

تاریخ دریافت: ۱۴۰۴/۸/۷ تاریخ پذیرش: ۱۴۰۴/۱۱/۲۷

چکیده

سمیت تخمدانی القاشده با دوکسوروبیسین (DOX) یکی از عوارض شایع شیمی‌درمانی در بیماران مبتلا به سرطان پستان است که اغلب با آسیب سلول‌های تخمدانی همراه بوده و منجر به آپوپتوز، اختلال در فولیکولوژنز و کاهش تولید هورمون‌های استروئیدی تخمدان می‌شود. دی‌متیل‌ایتاکونات (DMI)، یک متابولیت ایمنی با خواص ضدالتهابی و آنتی‌اکسیدانی است که می‌تواند اثرات محافظتی بالقوه‌ای داشته باشد، اما اطلاعات محدودی در مورد نقش محافظتی آن در برابر سمیت تخمدانی ناشی از شیمی‌درمانی وجود دارد. هدف از این مطالعه بررسی اثرات محافظتی احتمالی DMI بر تغییرات بافتی، آپوپتوز و تولید هورمون‌های جنسی در مدل موشی سرطان پستان 4T1 تحت درمان با DOX است. در این مطالعه تجربی، ۳۰ موش ماده بالغ نژاد BALB/c به صورت تصادفی به پنج گروه تقسیم شدند: کنترل سالم، کنترل سرطانی (القا سرطان با تزریق سلول‌های 4T1)، سرطان - DMI (50 mg/kg، تزریق داخل صفاقی، روزانه، ۲۸ روز)، سرطان - DOX (5 mg/kg، تزریق داخل صفاقی، هفته‌ای یک‌بار، ۴ هفته) و سرطان - DMI+DOX. سطوح سرمی استروژن و پروژسترون، بیان ژن‌های آپوپتوتیک تخمدان و تغییرات بافت تخمدان ارزیابی شد و با روش الایزا اندازه‌گیری شد. برای تحلیل آماری داده‌ها از نرم‌افزار GraphPad Prism نسخه ۱۰ استفاده شد و نتایج به صورت میانگین ± خطای معیار (Mean ± SEM) ارائه گردید. دوکسوروبیسین سطوح استرادیول (۳۷/۴+۲۳/۴۳ pg/ml) و پروژسترون (۳/۰+۴/۲ ng/ml) را به طور معنی‌داری کاهش داد و نیز موجب کاهش بیان Bcl2 (۰/۳۱ + ۰/۱)و افزایش بیان Bax (۴/۰+۰۴/۳۹) در بافت تخمدان، در مقایسه با گروه کنترل سرطانی شد (به ترتیب ۵۴/۲+۱۰/۸ pg/ml، ۵/۰+۱/۲ ng/ml، ۰/۰+۷۲/۰۹، ۱/۰+۸۱/۳۵). درمان همزمان **دی‌متیل‌ایتاکونات و دوکسوروبیسین** منجر به کاهش معنی‌دار Bax (۲/۵۹+۰/۴۵) و افزایش معنی‌دار Bcl-2 (۰/۶۱+۰/۰۳) نسبت به گروه دریافت‌کننده دوکسوروبیسین به تنهایی شد. همچنین، تغییرات بافتی قابل‌توجهی در بافت تخمدان از جمله افزایش آترزی فولیکولی، کاهش اندازه فولیکول‌ها و عدم وجود جسم زرد مشاهده شد. تجویز DMI سبب کاهش اختلالات بافتی و بهبود ساختار بافتی تخمدان، کاهش ضخامت اپی‌تلیوم سطحی و نرمال‌سازی سطوح هورمونی و بیان ژن‌های مرتبط با آپوپتوز گردید. درمان هم‌زمان با DMI و DOX بیش‌ترین اثر حفاظتی را در کاهش آسیب‌های بافتی ناشی از DOX نشان داد. نتایج این مطالعه نشان می‌دهد که DMI می‌تواند به عنوان ترکیبی محافظتی در کاهش سمیت تخمدانی در دوره شیمی درمانی مطرح باشد.

کلمات کلیدی: دی‌متیل‌ایتاکونات، دوکسوروبیسین، بافت‌شناسی تخمدان، آپوپتوز، سرطان سینه

* نویسنده مسئول: شیما حسینی‌فر، دانشیار گروه علوم پایه، دانشکده دامپزشکی، دانشگاه شهید چمران اهواز، اهواز، ایران
E-mail: sh.hosseinifar@suc.ac.ir

© 2020 by the authors. Licensee SCU, Ahvaz, Iran. This article is an open access article distributed under the terms and conditions of the Creative Commons Attribution-NonCommercial 4.0 International (CC BY-NC 4.0 license) (http://creativecommons.org/licenses/by-nc/4.0/).